Z. Phys. C – Particles and Fields 50, 1–10 (1991)

Zeitschrift für Physik C Particles and Fields

Observation of spin-parity 2^+ dominance in the reaction $\gamma\gamma \to \rho^0 \rho^0$ near threshold

ARGUS Collaboration

H. Albrecht, H. Ehrlichmann, R. Gläser, G. Harder, A. Krüger, A. Nau, A.W. Nilsson, A. Nippe, T. Oest, M. Reidenbach, M. Schäfer, W. Schmidt-Parzefall, H. Schröder, H.D. Schulz, F. Sefkow, R. Wurth

Desy, Hamburg, Federal Republic of Germany

R.D. Appuhn, A. Drescher, C. Hast, G. Herrera, H. Kolanoski, A. Lange, A. Lindner, R. Mankel, H. Scheck, M. Schieber, G. Schweda, B. Spaan, A. Walther, D. Wegener

Institut für Physik[1], Universität Dortmund, Federal Republic of Germany

M. Paulini, K. Reim, U. Volland, H. Wegener

Physikalisches Institut[2], Universität Erlangen-Nürnberg, Federal Republic of Germany

W. Funk, F. Heintz, J. Stiewe, S. Werner

Institut für Hochenergiephysik[3], Universität Heidelberg, Federal Republic of Germany

S. Ball, J.C. Gabriel, C. Geyer, A. Hölscher, W. Hofmann, B. Holzer S. Khan, J. Spengler

Max-Planck-Institut für Kernphysik, Heidelberg, Federal Republic of Germany

D.I. Britton[4], C.E.K. Charlesworth[5], K.W. Edwards[6], H. Kapitza[6], P. Krieger[5], R. Kutschke[5], D.B. MacFarlane[4], K.W. McLean[4], R.S. Orr[5], J.A. Parsons[5], P.M. Patel[4], J.D. Prentice[5], S.C. Seidel[5], J.D. Swain[5], G. Tsipolitis[4], K. Tzamariudaki[4], T.-S. Yoon[5]

Institute of Particle Physics[7], Canada

T. Ruf, S. Schael, K.R. Schubert, K. Strahl, R. Waldi, S. Weseler

Institut für Experimentelle Kernphysik[8], Universität, Karlsruhe, Federal Republic of Germany

B. Boštjančič, G. Kernel, P. Križan[9], E. Križnič, M. Pleško[10], T. Živko

Institut J. Stefan and Oddelek za fiziko[11], Univerza v Ljubljani, Ljubljana, Yugoslavia

H.I. Cronström, L. Jönsson

Institute of Physics[12], University of Lund, Sweden

A. Babaev, M. Danilov, B. Fominykii, A. Golutvin, I. Gorelov, V. Lubimov, A. Rostovtsev, A. Semenov, S. Semenov, V. Shevchenko, V. Soloshenko, V. Tchistilin, I. Tichomirov, Yu. Zaitsev

Institute of Theoretical and Experimental Physics, Moscow, USSR

R. Childers, C.W. Darden

University of South Carolina[13], Columbia, SC, USA

Received 29 October 1990

[1] Supported by the German Bundesministerium für Forschung und Technologie, under contract number 054DO51P
[2] Supported by the German Bundesministerium für Forschung und Technologie, under contract number 054ER12P
[3] Supported by the German Bundesministerium für Forschung und Technologie, under contract number 054HD24P
[4] McGill University, Montreal, Quebec, Canada
[5] University of Toronto, Toronto, Ontario, Canada
[6] Carleton University, Ottawa, Ontario, Canada
[7] Supported by the Natural Sciences and Engineering Research Council, Canada
[8] Supported by the German Bundesministerium für Forschung und Technologie, under contract number 054KA17P
[9] Supported by Alexander v. Humboldt Stiftung, Bonn
[10] Present address: Sincrotrone Trieste, I-34012 Trieste, Italy
[11] Supported by Raziskovalna skupnost Slovenije and the Internationales Büro KfA, Jülich
[12] Supported by the Swedish Reserach Council
[13] Supported by the U.S. Department of Energy, under contract DE-AS09-80ER10690

Abstract. The reaction $\gamma\gamma \to \pi^+ \pi^- \pi^+ \pi^-$ has been studied with the ARGUS detector. The rate in the invariant mass region below 1.8 GeV/c^2 is found to be largely due to $\rho^0 \rho^0$ production. A spin-parity analysis shows a dominance of the partial wave $(J^P, J_z) = (2^+, 2)$ with a small admixture from $J^P = 0^+$. The contribution of negative parity states is consistent with zero. The large ratio of cross sections $\sigma(\gamma\gamma \to \rho^0 \rho^0)/\sigma(\gamma\gamma \to \rho^+ \rho^-) \simeq 4$, and the dominance of the $J^P = 2^+$ wave in the reaction $\gamma\gamma \to \rho^0 \rho^0$ is a signature consistent with the production of an exotic $(I=2)$ resonance.

I Introduction

The reaction $\gamma\gamma \to \rho^0 \rho^0$ has been shown to have a large cross section in the region of the nominal $\rho^0 \rho^0$ threshold at approximately 1.5 GeV [1–6]. Such an enhancement is surprising since the rate should normally be strongly suppressed in the threshold region due to the reduced phase space. At the same time, the cross section for the isospin related reaction $\gamma\gamma \to \rho^+ \rho^-$ is at least a factor of four smaller [7, 8].

A simple isospin argument provides an important constraint on the origin of this difference. The two ρ^0 mesons can only be in a state with $I=0$, $I=2$ or some mixture of the two. The large ratio of the $\rho^0 \rho^0$ to $\rho^+ \rho^-$ cross sections cannot be accounted for by pure $I=0$ or pure $I=2$ states, bute can only result from interference between the two isospin states. The interference is observed to be constructive in $\gamma\gamma \to \rho^0 \rho^0$ and destructive $\gamma\gamma \to \rho^+ \rho^-$. This basic argument leaves open the question of the dynamics of $\rho\rho$ production by two photons. Attempts have been made to explain this either by dominantly resonant [9] or non-resonant [10] mechanisms. A demonstration that the $\rho\rho$ cross section is predominantly resonant in origin, together with the isospin argument given above, would imply the existence of exotic $(I=2)$ states, such as $qq\overline{qq}$ resonances. It is therefore important to make a thorough partial-wave analysis of the process.

Unfortunately, it is exactly in performing partial-wave studies of $\gamma\gamma \to \rho^0 \rho^0$ where previous experiments have failed to give a consistent answer. In general, the results agree only on the dominance of positive-parity states [3, 5, 6]. In this study we attempt to resolve differences in the partial-wave decomposition using a high-statistics data sample collected by the ARGUS experiment at $e^+ e^-$ center-of-mass energies around 10 GeV. In comparison with the PETRA and PEP experiments, the lower beam energies in DORIS result in smaller boosts of the $\gamma\gamma$ system along the beam axis, which, together with a good angular acceptance for charged tracks, increases our ability to discriminate among different spin-parity (J^P) states of the $\rho^0 \rho^0$ system.

This paper is organized as follows. In Sect. II we present the data selection criteria and estimate the possible backgrounds. Section III contains a description of the model used in the spin-partity analysis and of the maximum likelihood method. The determination of cross sections is given in Sect. IV. In Sect. V the systematic uncertainties in the analysis are discussed in detail. We conclude in Sect. VI with a summary.

II Data selection and background estimation

The two-photon production of four pions, $\gamma\gamma \to \pi^+ \pi^- \pi^+ \pi^-$, is observed in $e^+ e^-$ storage rings via the reaction

$$e^+ e^- \to e^+ e^- \pi^+ \pi^- \pi^+ \pi^-.$$

The final state electron and positron predominantly scatter at low angles and escape detection (no-tag experiments). The data used for the study of this reaction were taken at an average $e^+ e^-$ center-of-mass energy of 10.2 GeV and correspond to an integrated luminosity of 242 pb^{-1}. The ARGUS detector, its trigger and particle identification capabilities have been described elsewhere [11]. For event selection we required exactly four charged particles, with zero net charge, originating from a common event vertex. In addition, each particle had to be consistent with the pion mass hypothesis, by requiring the combined likelihood ratio from specific ionization and time-of-flight measurements to exceed 1%. For the polar angle between the charged particle and the beam axis we required $|\cos\theta| \leqq 0.92$, and for the transverse momentum $p_t \geqq 50$ MeV/c. In the accepted range the efficiency is almost independent of $\cos\theta$, while it increases with p_t and reaches 50% (80%) of the plateau value at 100 MeV/c (200 MeV/c).

To further enhance exclusive $\gamma\gamma \to \pi^+ \pi^- \pi^+ \pi^-$ events we required the net transverse momentum, $|\Sigma \mathbf{p}_t|$, to be smaller than 0.12 GeV/c and the sum of scalar momenta, $\Sigma|\mathbf{p}|$, to be less than 4 GeV/c. In addition, no photon candidates with energy deposition in the electromagnetic calorimeter greater than 50 MeV were allowed in the event. After applying these cuts a sample of 5701 events was obtained, out of which 5181 lie in the invariant mass region between 1.1 and 2.3 GeV/c^2 (Fig. 1).

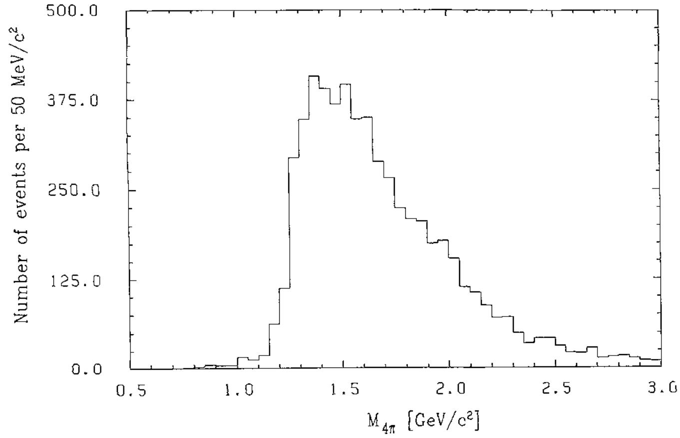

Fig. 1. Invariant mass distribution of accepted $\pi^+ \pi^- \pi^+ \pi^-$ events

Possible background from τ decays was estimated using Monte Carlo simulated $e^+e^- \to \tau^+\tau^-$ events. Scaling the number of τ events to the luminosity of the data sample, we estimate the background from τ decays to be 3 events in the $\gamma\gamma$ invariant mass region below 2.3 GeV/c^2. The background from incompletely reconstructed events of the type $e^+e^- \to$ hadrons, was estimated in a similar way to be 2 events. The background from the reaction $\gamma\gamma \to \pi^+\pi^-\pi^+\pi^-\pi^0$, where photons from the π^0 decay were not detected, was estimated to be 42 events using a Monte Carlo simulation, normalized to the measured topological cross section for this reaction [12].

The feeddown contribution from $\gamma\gamma \to N\pi$ events ($N \geqq 6$), where two or more pions were not reconstructed, was estimated from the $|\Sigma \mathbf{p}_t|^2$ distribution. The shape of the $|\Sigma \mathbf{p}_t|^2$ spectra for $\gamma\gamma \to \pi^+\pi^-\pi^+\pi^-$ and $\gamma\gamma \to \pi^+\pi^-\pi^+\pi^-\pi^0$ (with a missing π^0) events was determined by Monte Carlo simulation. A fit to the data was performed using this predicted spectrum, plus a constant term to describe any remaining background. The $|\Sigma \mathbf{p}_t|^2$ distribution of $\pi^+\pi^-\pi^+\pi^-$ events was thereby found to be consistent with the assumption that all events originate only from exclusive four-pion final states and the estimated five-pion background. A background with a flat $|\Sigma \mathbf{p}_t|^2$ distribution contributes less than 46 events to our final samples, at the 90% confidence level. This procedure also takes into account the background originating from τ decays and from events of the type $e^+e^- \to$ hadrons.

In total, we estimated the background from the processes $e^+e^- \to \tau^+\tau^-$ und $e^+e^- \to$ hadrons to be 5 events and the background from the reaction $\gamma\gamma \to \pi^+\pi^-\pi^+\pi^-\pi^0$, where the π^0 is not detected, to be 42 events. The feeddown contribution from the reaction $\gamma\gamma \to N\pi$ ($N \geqq 6$) is less than 41 events (90% c.l.).

III Analysis of the $\pi^+\pi^-\pi^+\pi^-$ final state and the maximum likelihood method

Most of the measured $\pi^+\pi^-\pi^+\pi^-$ events have invariant masses in the region between 1 and 2 GeV/c^2 (Fig. 1). The invariant mass distribution peaks just below the nominal $\rho^0\rho^0$ threshold. The TASSO collaboration [1] first observed that the final state in $\gamma\gamma \to \pi^+\pi^-\pi^+\pi^-$ consists mainly of $\rho^0\rho^0$, for $\gamma\gamma$ invariant masses, $W_{\gamma\gamma}$, below 1.8 GeV/c^2. This result has been confirmed by other measurements [2–6].

In analyzing the reaction $\gamma\gamma \to \pi^+\pi^-\pi^+\pi^-$ we allow for $\rho^0\rho^0$ production in different (J^P, J_z) states, as well as for incoherent contributions of $\rho^0\pi^+\pi^-$ and $\pi^+\pi^-\pi^+\pi^-$. The latter two processes are taken to be uniformly distributed in phase space. As has been pointed out in [9], this assumption is unphysical in the case of $\gamma\gamma \to \rho^0\pi^+\pi^-$. However, our study shows that phase-space distributed contributions of $\rho^0\pi^+\pi^-$ and $\pi^+\pi^-\pi^+\pi^-$ are able to acount for those final states which cannot be described by $\rho^0\rho^0$ production. The effect of the presence of an unphysical $\rho^0\pi^+\pi^-$ state on the results of the $\rho^0\rho^0$ partial-wave analysis is discussed in Sect. V.

The final states in no-tag $\gamma\gamma$ reactions are constrained to even spins with helicity $J_z = 0$, and to $J^P = 2^+, 3^+, 4^+, \ldots$ states with helicity $J_z = \pm 2$ (z axis in $\gamma\gamma$ direction) [13]. If we assume that for $W_{\gamma\gamma}$ below 2 GeV/c^2 the only important $\rho^0\rho^0$ states are those with spin $J \leqq 2$, we are left with five different possible spin-parities (J^P, J_z) = 0^+, 0^-, (2^+, ± 2), (2^+, 0) and 2^-. The wave function describing the rotational properties of a certain J^P state is constructed by first combining the spin of the two ρ^0 mesons $\mathbf{j} = \mathbf{j}_1 + \mathbf{j}_2$, and then by adding the orbital angular momentum $\mathbf{L}$ to obtain the total spin $\mathbf{J} = \mathbf{j} + \mathbf{L}$:

$$\Psi^{L,j}_{J^P,J_z}(1,2) = \sum_{(m+M=J_z)} \sum_{(m_1+m_2=m)} \cdot C^{JJ_z}_{jm,LM}\, C^{jm}_{j_1m_1,j_2m_2}\, Y^M_L(\theta,\phi)\, Y^{m_1}_{j_1}(\theta_1,\phi_1)\, Y^{m_2}_{j_2}(\theta_2,\phi_2),$$

where θ, ϕ are the polar and the azimuthal angles of the ρ^0 meson in a coordinate system with the z axis along the $\gamma\gamma$ axis ($\gamma\gamma$ helicity system), which for the no-tag reaction, to a good approximation, coincides with the beam axis. The angles θ_1, ϕ_1 (θ_2, ϕ_2) define the direction of the $\pi^+_{1(2)}$ in the center-of-mass system of the first (second) ρ^0. Both ρ^0 systems have coordinate axes parallel to those of the $\gamma\gamma$ helicity system. The C's are the appropriate Clebsch-Gordon coefficients.

The possible values of $\rho^0\rho^0$ orbital angular momenta are $L=1$ for $J^P = 0^-$, $L = 0,2$ for $J^P = 0^+$, $L = 1,3$ for $J^P = 2^-$, and $L = 0, 2, 4$ for $J^P = 2^+$. Since the analysis of the reaction $\gamma\gamma \to \rho^0\rho^0$ is performed close to threshold we feel justified in restricting the orbital angular momenta to $L=0$ and $L=1$. For a hard-sphere scattering model with an interaction radius of 1 fm, for example, higher values of L become important only in the $W_{\gamma\gamma}$ region above 1.8 GeV/c^2 [14]. Note that in the case of $L=0$ or $L=1$, the spin $\mathbf{j}$ of the two ρ^0 mesons is also unique, so that we will drop the wave function indices L and j in the following.

In order to describe $\pi^+\pi^-\pi^+\pi^-$ production by two photons we define amplitudes for $\rho^0\rho^0$ production in the different (J^P, J_z) states and amplitudes for isotropic $\rho^0\pi^+\pi^-$ and $\pi^+\pi^-\pi^+\pi^-$ states. Four particles in their center-of-mass system are described by seven kinematical variables. We used five of the angles defined above (the angle ϕ is redundant in a no-tag experiment) and the two invariant masses of the oppositely charged pions ($m_{\pi^+\pi^-} \equiv m_{\rho^0}$). Apart from factors dependent on $W_{\gamma\gamma}$ the amplitudes read:

(a) $\rho^0\rho^0$ production:

$$T^{J^P,J_z}_{\rho^0\rho^0} = \mathrm{RBW}(m_{\rho^0_1})\, \mathrm{RBW}(m_{\rho^0_2})\, \Psi_{J^P,J_z}(1,2) + \text{permutation},$$

(b) isotropic $\rho^0\pi^+\pi^-$ production:

$$T_{\rho^0\pi^+\pi^-} = \mathrm{RBW}(m_{\rho^0}) + \text{permutations},$$

(c) isotropic $\pi^+\pi^-\pi^+\pi^-$ production:

$$T_{4\pi} = 1,$$

where $\mathrm{RBW}(m_{\rho^0})$ is the relativistic Breit-Wigner amplitude for the ρ^0 resonance [3, 15]. The permutations symmetrize the matrix elements with respect to identical pions, since four $\rho^0 \pi^+ \pi^-$ and two $\rho^0 \rho^0$ combinations are possible in a single $\pi^+ \pi^- \pi^+ \pi^-$ event. For the $\rho^0 \rho^0$ state with $J^P = 2^+$ the interference term arising from this symmetrization makes it possible to distinguish helicity +2 from helicity −2. However, in our analysis we find that the corresponding angular distributions are too similar to allow for a separate determination of each helicity contribution. Henceforth, the helicity +2 state will represent the sum of both helicities.

The probability that a measured event originates from a certain process is proportional to the square of the corresponding amplitude. The only $\rho^0 \rho^0$ states which can interfere are those with equal parity and equal helicity [13]. As a consequence, the square of the sum of the amplitude $J^\pi = 2^+$ with helicity 0, and the amplitude $J^P = 0^+$, enters the expression for the cross section. The same holds for the sum of $J^P = 0^-$ and $J^P = 2^-$ amplitudes (note that $J^P = 2^-$ with helicity 2 is absent).

Using these amplitudes the logarithm of a likelihood function is defined as follows:

$$\ln L = \sum_{i=1}^{N} \ln \sum_{k,r} P_{k,r} \lambda_k \lambda_r M_k(i) M_r^*(i) - N \int [\sum_{k,r} P_{k,r} \lambda_k \lambda_r M_k(x) M_r^*(x)] \, \eta(x) \Phi(x) \omega_4(x) \, dx,$$

$$\text{where } M_k(i) = \frac{T_k(i)}{\sqrt{\overline{|T_k|^2}}},$$

where the index i runs over all measured events in the $W_{\gamma\gamma}$ bin. The diagonal elements of the Hermitian matrix P are equal to one, while the only non-zero off-diagonal elements are $P_{0^+,(2^+,0)} = \exp(i\delta_+)$ and $P_{0^-,2^-} = \exp(i\delta_-)$. The normalization integral and the average of the square of the matrix element, $\overline{|T_k|^2}$, are calculated using a Monte Carlo method. Both integrations are performed over the acceptance $\eta(x)$, where x represents the variables describing the four pions in their system as well as the kinematical variables describing the two photons. The four-momenta of the $\gamma\gamma$ system were generated according to the exact expression for the transverse $\gamma\gamma$ luminosity function $\Phi(x)$ [16]. The generation of pion momentum vectors was performed according to the particle phase-space density $\omega_4(x)$. A program [11], which simulates in detail the ARGUS detector was used to process the events. The procedure included a trigger simulation, and the same selection criteria as applied to the data.

The seven parameters λ_k and the two relative phases, δ_+ and δ_-, are obtained by requiring a maximum value for the likelihood function. In the case of non-interfering amplitudes, where λ_k^2 represents the fraction of measured events which belongs to the process k, we have varied λ_k^2 and not λ_k, so that the procedure does not exclude negative fractions.

IV Determination of the cross sections

A fit to the data was performed using nine free parameters: seven amplitudes λ_k and two relative phases δ_+ and δ_-. However, the results of this procedure were consistent with those obtained using a seven parameter fit where the interferences were neglected. The reason is that over the whole $W_{\gamma\gamma}$ range the negative parity amplitudes 0^- and 2^-, as well as the $(2^+, 0)$ amplitude, were small, leading to negligible interference terms. Note that a measurement of the $W_{\gamma\gamma}$ dependence of the phases δ_+ or δ_- could provide a tool for testing the presence of resonances. Unfortunately, because the $(2^+, 0)$ amplitude is small, it seems unlikely, even in an experiment with much better statistics, that the $W_{\gamma\gamma}$ dependence of the phase δ_+ could be measured.

The cross section for the process k averaged over a $W_{\gamma\gamma}$ bin is calculated using the following formula:

$$\sigma_{\gamma\gamma \to k} = \frac{N \lambda_k^2}{\eta_k \varepsilon} \frac{1}{L_{ee}} \frac{1}{\frac{\Delta L}{\Delta W_{\gamma\gamma}} \Delta W_{\gamma\gamma}},$$

where N is the number of events in the $\Delta W_{\gamma\gamma}$ bin, L_{ee} is the integrated $e^+ e^-$ luminosity and $\Delta L / \Delta W_{\gamma\gamma}$ is the differential $\gamma\gamma$ luminosity function. The acceptances are given as products of the two terms η_k and ε [17]. The efficiency for the selection requirement that no photons are detected in the event (see Sect. II) is found to be $\varepsilon = 0.56 \pm 0.03$, and is within the error independent of $W_{\gamma\gamma}$ and the process considered. The detector and trigger efficiences, as well as the efficiences for the remaining selection requirements, are described by η_k (Fig. 2).

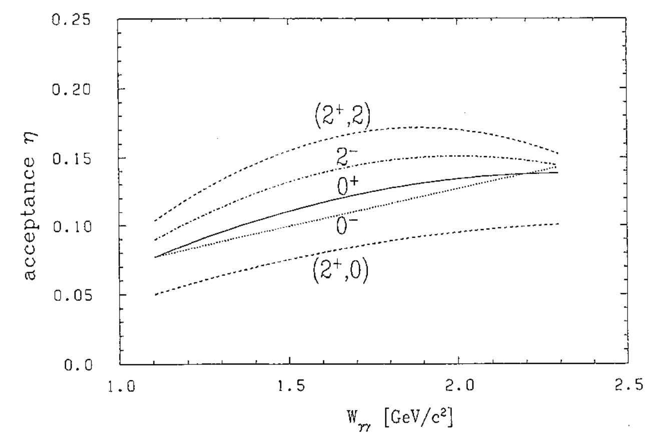

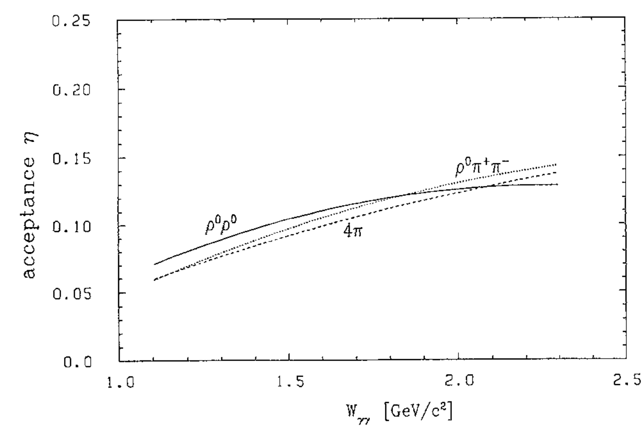

Fig. 2. Acceptances η_k for various $\rho^0 \rho^0$ spin-parity states (J^P, J_z), and for the isotropic $\rho^0 \rho^0$, $\rho^0 \pi^+ \pi^-$ and $\pi^+ \pi^- \pi^+ \pi^-$ states. Combined statistical and systematic errors on the accpetances are 8%

The results of the analysis in 100 MeV/c^2 bins of $W_{\gamma\gamma}$ are given in Table 1. The cross section for the $J^P=2^+$ with helicity 2 wave is dominant. The contribution from negative 0^- and 2^- is small. The helicity 0 component of $J^P=2^+$ is suppressed with respect to helicity 2, as is also observed for tensor meson production in $\gamma\gamma$ reactions. The analysis was also performed using 50 MeV/c^2 wide bins in $W_{\gamma\gamma}$. The results of the two cases are consistent within errors (Fig. 3).

It is interesting that some of the one-dimensional distributions alone provide a means of distinguishing between the various J^P states. There are two relative angles which are only weakly affected by the acceptance. From the distribution of the angle ϑ between the directions of the π^+ from the first and the π^+ from the second ρ^0, each direction measured in its own center-of-mass system, it is possible to distinguish $J^P=0^+$ from $J^P=2^+$ (Fig. 4a). On the other hand, the distribution of the angle χ between the two ρ^0 decay planes is sensitive to the parity of the amplitudes (Fig. 4b). Neglecting the width of the ρ^0, the χ distributions are $dN/d\chi \propto (1+\alpha\cos 2\chi)$, where $\alpha=-1$ for $J^P=0^-$ and $\alpha=2/3$ for $J^P=0^+$. For other spin-parity states the values of α lie between these two extremes. However, the wave function symmetrization for ρ^0 mesons with finite width (two possible $\rho^0\rho^0$ combinations per event) spoils the symmetry around $\chi=90°$, an effect which decreases with increasing $\rho^0\rho^0$ center-of-mass energy $W_{\gamma\gamma}$. For the same reason the angular distribution $dN/d\cos\vartheta$ is also asymmetric. This asymmetry in the distributions of the anglex χ and ϑ was not noticed by previous experiments [3, 5, 6].

In order to demonstrate that the model defined above describes the data well, we show as examples the one dimensional angular distributions $\cos\vartheta$ and χ, along with the two-pion invariant mass distributions $m_{\pi^+\pi^-}$ and $m_{\pi^\pm\pi^\pm}$ (Fig. 5). The ρ shape in the $m_{\pi^+\pi^-}$ distribution is particularly well described by the model. The chi-square values for the $m_{\pi^+\pi^-}$, $m_{\pi^\pm\pi^\pm}$, $\cos\vartheta$ and χ distributions are given in Table 2 for various $W_{\gamma\gamma}$ intervals.

Table 1. Cross sections (in nanobarns) for various J^P states of $\rho^0\rho^0$, and for the $\rho^0\pi^+\pi^-$ and $\pi^+\pi^-\pi^+\pi^-$ states (assuming phase-space distribution), as obtained by a 7 parameter fit. Also given is the sum of the cross sections over all J^P states of $\rho^0\rho^0$. The errors shown are statistical only. Note that care has to be taken when adding up different contributions because the errors on the cross sections in certain $W_{\gamma\gamma}$ bins are correlated

$W_{\gamma\gamma}$ (GeV/c^2)	0^+	0^-	$(2^+, 2)$	$(2^+, 0)$
1.2–1.3	10.1 ± 3.8	4.4 ± 1.5	21.6 ± 4.0	-5.0 ± 3.3
1.3–1.4	15.2 ± 3.7	3.3 ± 2.2	42.7 ± 3.0	-2.9 ± 5.2
1.4–1.5	17.2 ± 5.5	2.5 ± 2.6	45.5 ± 6.2	2.1 ± 4.6
1.5–1.6	10.2 ± 5.3	-1.1 ± 2.7	56.8 ± 5.6	-10.4 ± 3.5
1.6–1.7	4.0 ± 5.2	3.9 ± 2.9	52.5 ± 5.7	3.5 ± 4.0
1.7–1.8	10.1 ± 5.1	0.9 ± 2.7	35.4 ± 5.3	0.7 ± 4.1
1.8–1.9	-11.8 ± 5.0	7.7 ± 2.8	34.7 ± 5.1	4.5 ± 3.5
1.9–2.0	2.9 ± 4.3	4.2 ± 2.7	18.5 ± 4.6	2.8 ± 3.9
2.0–2.1	-5.8 ± 2.7	0.3 ± 2.2	19.6 ± 2.6	4.7 ± 3.9
2.1–2.2	2.4 ± 3.5	-0.1 ± 1.5	4.6 ± 4.0	4.4 ± 3.6

$W_{\gamma\gamma}$ (GeV/c^2)	2^-	$\rho^0\pi^+\pi^-$	$\pi^+\pi^-\pi^+\pi^-$	$\Sigma\rho^0\rho^0$
1.2–1.3	-0.5 ± 1.9	11.8 ± 4.8	2.1 ± 3.3	30.6 ± 2.0
1.3–1.4	0.4 ± 2.4	9.2 ± 5.4	18.7 ± 4.5	58.9 ± 2.4
1.4–1.5	1.8 ± 3.0	3.1 ± 5.4	18.8 ± 4.0	69.4 ± 2.6
1.5–1.6	2.9 ± 2.8	3.2 ± 3.8	25.5 ± 3.4	58.6 ± 3.6
1.6–1.7	-0.2 ± 3.1	0.9 ± 6.4	19.7 ± 3.9	63.9 ± 3.7
1.7–1.8	-2.0 ± 2.9	13.8 ± 6.6	13.4 ± 3.6	45.3 ± 4.3
1.8–1.9	-6.5 ± 2.5	20.2 ± 8.2	20.8 ± 4.0	28.8 ± 5.3
1.9–2.0	-1.6 ± 2.2	12.1 ± 7.9	27.7 ± 4.5	26.9 ± 5.1
2.0–2.1	-2.6 ± 1.8	9.0 ± 6.1	29.5 ± 4.1	16.1 ± 3.8
2.1–2.2	2.3 ± 2.0	10.5 ± 5.4	20.3 ± 3.9	13.6 ± 3.2

V Determination of systematic errors

It is particularly important for a spin-parity analysis to have a detector which covers as much of the solid angle as possible. Some of the partial waves, such as 0^+ and 2^+, are difficult to distinguish because of the low acceptance in the forward region. The dominance of the 2^+ partial wave observed in our data is consistent with the results in [6]. However, they found equal contributions of the $(2^+, 2)$ and $(2^+, 0)$ amplitudes, by fitting histograms, as opposed to the unbinned analyses used in [3, 5] and in this paper. In [5], roughly equal contributions of 2^+ and 0^+ amplitudes were obtained, while in [3] a dominance of 0^+ over 2^+ for $W_{\gamma\gamma}\leqq 1.7$ GeV/c^2 was found. In order to test whether 0^+ dominance is compatible with our data we repeated the likelihood fit with the $(2^+, 2)$ contribution constrained to zero. The fit compensates for the missing $(2^+, 2)$ component by increasing the 0^+, 2^- and $\rho^0\pi^+\pi^-$ contributions. However, the likelihood functions in the $W_{\gamma\gamma}$ range from 1.2 to 1.8 GeV/c^2 differ by about fifty from those of the best fit, excluding such a possibility at the 10 σ level. This conclusion is confirmed by the fact that the chi-square values obtained with this fit for distributions of $\cos\vartheta$ and χ increase by about 2.

We have investigated a possible explanation for the disagreement between various experiments. The values of λ_k^2 that correspond to the maximum of the likelihood function depend strongly on $\overline{|T_k|^2}$. It is essential to determine $\overline{|T_k|^2}$ with high precision for those amplitudes with similar distributions in the multidimensional space of the measured quantities. As an example, we present the results of our study in the $W_{\gamma\gamma}$ bin between 1.4 and 1.5 GeV/c^2, where the fraction values $\lambda^2_{(2^+,2)}=0.61$ and $\lambda^2_{0^+}=0.17$ were obtained. For variations of the $\overline{|T_{(2^+,2)}|^2}$ smaller than 5% following linear relation was found to hold:

$$\frac{\delta\lambda_k^2}{\lambda_k^2}\approx a_k\frac{\delta\overline{|T_{(2^+,2)}|^2}}{\overline{|T_{(2^+,2)}|^2}},$$

where $a_{(2^+,2)}=-7.1$ and $a_{0^+}=13.8$. A similar linear behaviour results from varying $\overline{|T_{0^+}|^2}$ where now the slopes are: $a_{(2^+,2)}=3.9$ and $a_{0^+}=-11.8$. Negative parity fractions as well as $\rho^0\pi^+\pi^-$ and $\pi^+\pi^-\pi^+\pi^-$ contributions are less sensitive to such variations, since these processes are only weakly correlated with $(2^+, 2)$ and 0^+. We conclude that small systematic or statistical er-

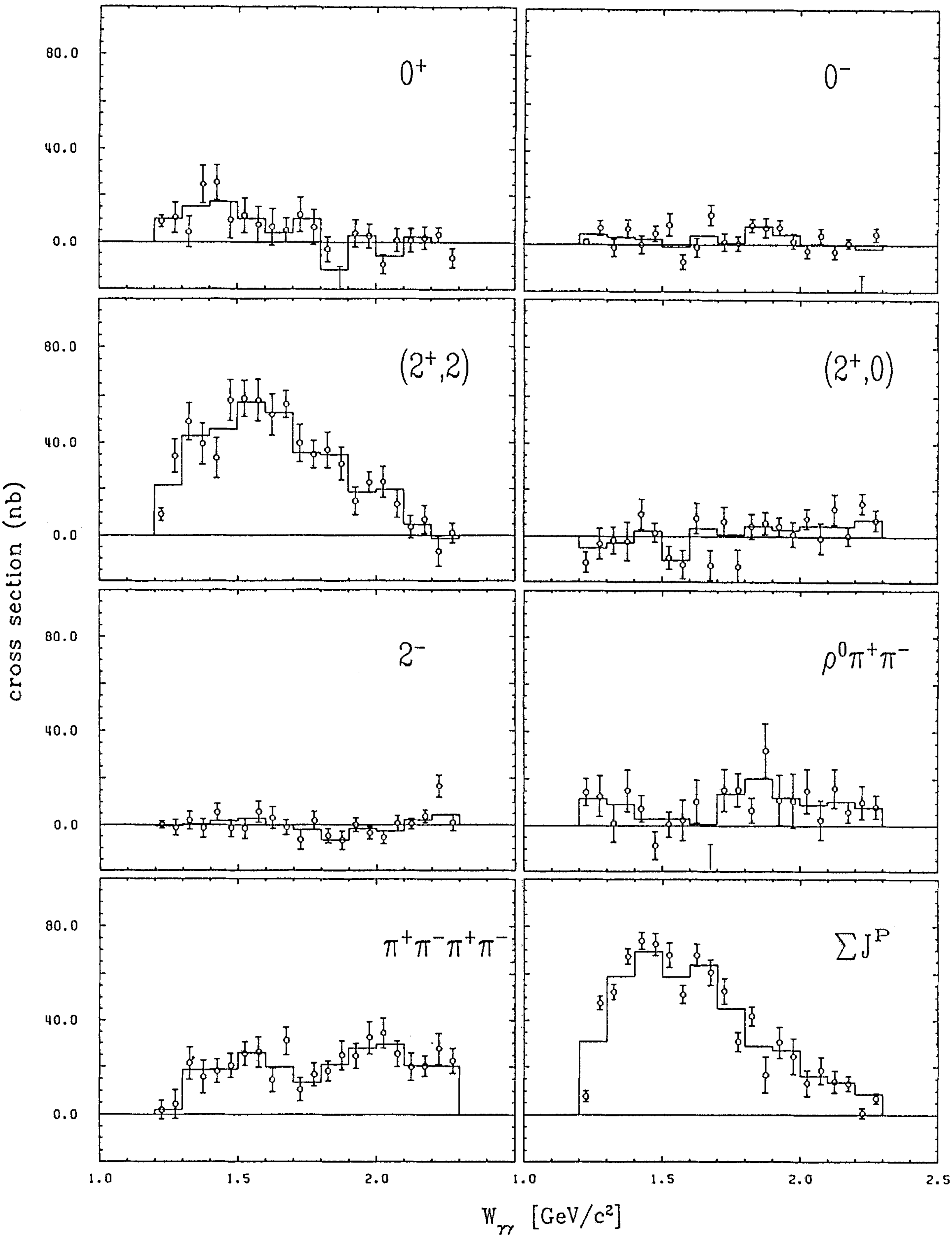

Fig. 3. Cross sections for different J^P states of $\rho^0\rho^0$, and for the $\rho^0\pi^+\pi^-$ and $\pi^+\pi^-\pi^+\pi^-$ states (assuming phase-space distribution), as determined by a 7 parameter fit in $W_{\gamma\gamma}$ bins of width 100 MeV/c^2 (histogram) and 50 MeV/c^2 (circles). Also shown is the sum of the cross sections over all J^P states of $\rho^0\rho^0$

rors on $\overline{|T_{(2^+,2)}|^2}$ or $\overline{|T_{0^+}|^2}$ could account for the differences in the $(2^+, 2)/0^+$ ratio among the experiments. At the same time this could also explain why all experiments agree on the smallness of negative parity contributions.

The combined statistical and systematic errors on the

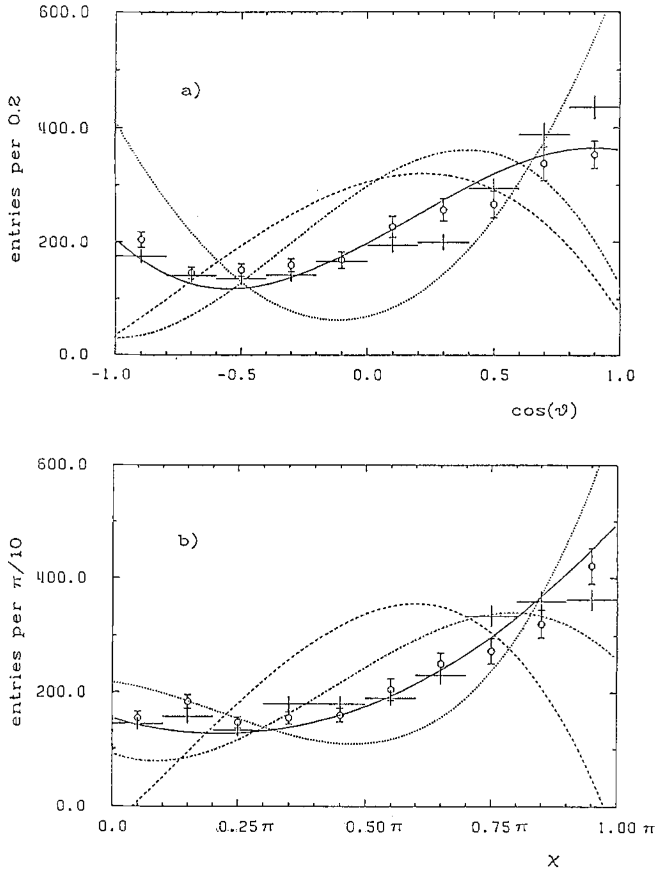

Fig. 4. One-dimensional angular distributions (the definition of the angles is given in the text) for $1.6 < W_{\gamma\gamma} < 1.8$ GeV/c^2. The result of a 7 parameter fit (circles) is compared to the data (crosses). Also shown are the simulated distributions for various $\rho^0\rho^0$ spin-parity states: $J^P = 0^+$ (dotted line), $J^P = 0^-$ (dashed line), $J^P = 2^+$ with helicity 2 (solid line) and $J^P = 2^-$ (dash-dotted line)

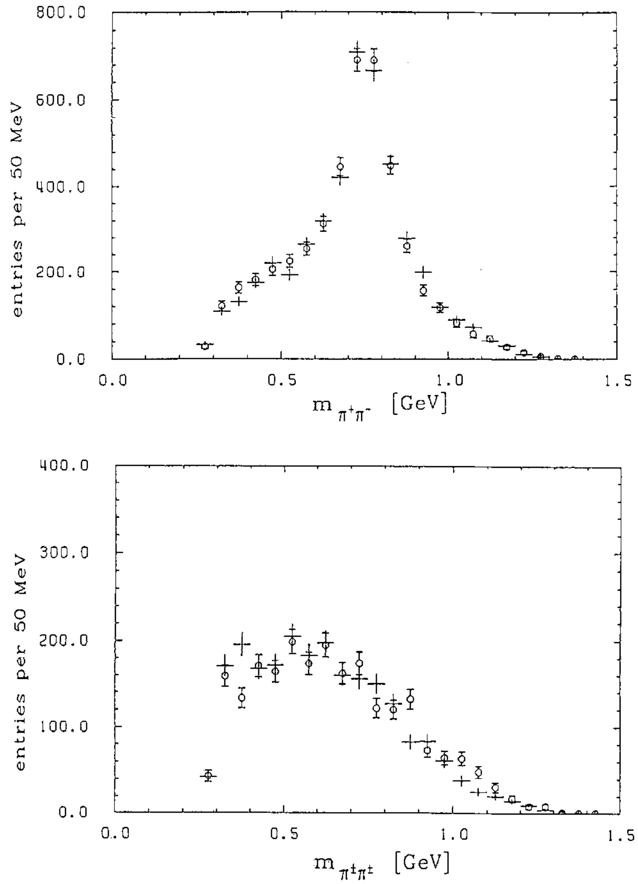

Fig. 5. Two-pion invariant mass distributions $m_{\pi^+\pi^-}$ (four entries per event) and $m_{\pi^\pm\pi^\pm}$ (two entries per event) for $1.6 < W_{\gamma\gamma} < 1.8$ GeV/c^2. The data (crosses) are compared to the results of a 7 parameter fit (circles)

acceptances η_k are 8%. Since only the ratio of the acceptances $\eta_k/\eta_{4\pi}$ is important for the determination of $\overline{|T_k|^2}$ and thus for the fractions λ_k^2, the uncertainties in the acceptances to a large extent cancel out. In our case the combined statistical and systematic error on $\overline{|T_k|^2}$ is 2.1% [17].

The stability of our results has been checked by dividing the $\pi^+\pi^-\pi^+\pi^-$ events into two samples, one with boost values $|cp_z|/W_{\gamma\gamma} \leq 0.32$, and the other with $|cp_z|/W_{\gamma\gamma} > 0.32$. Here p_z represents the component of the $\pi^+\pi^-\pi^+\pi^-$ momentum along the beam axis. The boost value of 0.32 was chosen to separate the data into two samples of about equal number of events. The acceptances and average matrix elements $\overline{|T_k|^2}$ were calculated for each data sample separately. For the low boost sample the acceptances for various J^P states do not differ as much as for the high boost sample. On the other hand, we expect that if there is a systematic uncertainty in $\overline{|T_k|^2}$ it is not the same for low and high boost values. For example, higher boosts mean that there are more charged tracks hitting the forward part of the spectrometer. Such changes in the event topology have an impact on the trigger acceptance [17]. A 7 parameter likelihood fit was performed on both samples. The results are shown in Fig. 6. The cross sections determined separately from

Table 2. The values for chi-square/N_d obtained from the comparison of the one dimensional angular and two-pion invariant mass distributions in the data with the results of a 7 parameter fit (see also Fig. 2). N_d is given (values in brackets) by the number of bins minus one for the overall normalisation

$W_{\gamma\gamma}$ (GeV/c^2)	$\cos\vartheta$	χ	$m_{\pi^+\pi^-}$	$m_{\pi^\pm\pi^\pm}$
1.2 – 1.4	1.65(9)	1.50(9)	3.22(14)	1.33(14)
1.4 – 1.6	1.70(9)	2.85(9)	0.85(16)	2.06(17)
1.6 – 1.8	2.25(9)	3.07(9)	0.91(20)	2.35(20)
1.8 – 2.0	2.90(9)	4.76(9)	1.53(24)	2.73(24)

the low- and high-boost data, are consistent within the errors, and agree with the results found in the complete data sample. From the comparison of the (2^+, 2) cross section for the low- and high-boost data, we determine the average systematic error per $W_{\gamma\gamma}$ bin for the (2^+, 2) cross section to be 14%. This is consistent with the direct estimate of the systematic errors on the average matrix elements $\overline{|T_k|^2}$.

In summary, the systematic error on the cross section of each contribution k is estimated by

$$\Delta\sigma_{\gamma\gamma\to k} = \sqrt{5^2 + (0.10\,\sigma_{\gamma\gamma\to}/\mathrm{nb})^2}\ \mathrm{nb},$$

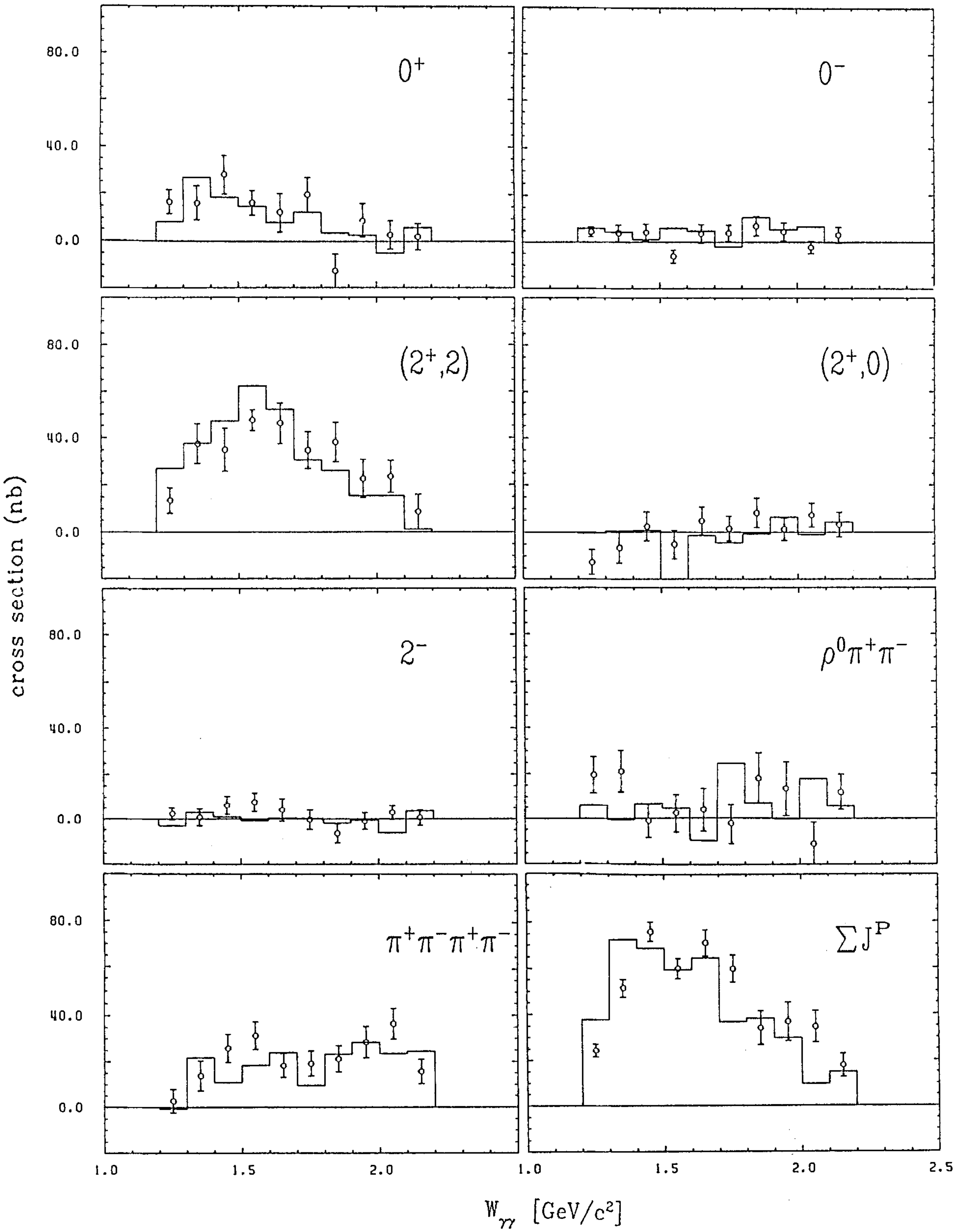

Fig. 6. Cross sections for different J^P states of $\rho^0\rho^0$ and for the $\rho^0\pi^+\pi^-$ and $\pi^+\pi^-\pi^+\pi^-$ states (assuming phase-space distribution), as determined by a 7 parameter fit for events with boost values below 0.32 (circles) and for events with boost values above 0.32 (histogram). Also shown are the corresponding sums of the cross sections over all J^P states of $\rho^0\rho^0$. The definition of the boost is given in the text

where the first term originates from the systematic errors on the fractions and the second term from the systematic errors on the acceptances and the integrated e^+e^- luminosity. The systematic error on the sum of the $\rho^0\rho^0$ cross sections is approximately given by

$$\Delta\sigma_{\rho^0\rho^0}=\sqrt{2.5^2+(0.10\,\sigma_{\rho^0\rho^0}/\mathrm{nb})^2}\ \mathrm{nb}.$$

The likelihood method was extensively tested using Monte Carlo events [17]. Event samples with different J^P compositions were used as input data and analyzed in the same way as the measured data. In all cases the input data were correctly reproduced. When the number of amplitudes was larger in the fitting procedure than in the input data, those amplitudes that were not included in the input data gave also no contribution. However, when some amplitudes were neglected in the analysis they would appear in the channels with the largest correlation coefficient. For example, neglecting 0^+ in the fit caused a migration to $(2^+, 2)$. We also studied the case where only phase-space distributed $\rho^0\rho^0$, $\rho^0\pi^+\pi^-$ and $\pi^+\pi^-\pi^+\pi^-$ configurations were allowed in the fit, while the input data contained several J^P states of $\rho^0\rho^0$ in addition to the phase-space distributed $\rho^0\pi^+\pi^-$ and $\pi^+\pi^-\pi^+\pi^-$. The result of the analysis shows that the isotropic $\rho^0\rho^0$ channel absorbs all J^P states of $\rho^0\rho^0$. In this context it should be noted that our data could also be well fitted with such an isotropic $\rho^0\rho^0$ hypothesis.

We now turn to the discussion of the $\rho^0\pi^+\pi^-$ contribution. C-parity requires the angular momentum between the two pions to be odd, thereby forbidding an isotropic angular distribution. It is thus necessary to check the migration of possible non-isotropic $\rho^0\pi^+\pi^-$ states. For this reason $\rho^0\rho^0$ and $\rho^0\pi^+\pi^-$ Monte Carlo events were taken as input data. Each was composed of three components: $J^P=2^+$ with helicity 2, $J^P=0^-$, and a component with an isotropic angular distribution. In the analysis, however, all three were included only for $\rho^0\rho^0$, while $\rho^0\pi^+\pi^-$ was restricted to the isotropic contribution. We found that the $(2^+, 2)$ and most of the 0^- $\rho^0\pi^+\pi^-$ events did indeed contribute to the isotropic $\rho^0\pi^+\pi^-$ channel, with only a small fraction of $J^P=0^-$ $\rho^0\pi^+\pi^-$ events migrating to the $J^P=0^-$ $\rho^0\rho^0$ channel. The same was true if the $(2^+, 2)$ and 0^- components were replaced instead by 0^+ and 2^-. It appears that the Breit-Wigner form of the invariant masses is more restrictive than the angular distributions. Thus, we conclude that the $\rho^0\pi^+\pi^-$ contribution can be reliably estimated using an isotropic angular distribution in the fit. The isotropic $\rho^0\pi^+\pi^-$ channel also absorbs possible contributions from the reaction $\gamma\gamma\to a_1(1260)^\pm\pi^\mp\to\rho^0\pi^\pm\pi^\mp$. The large width of the a_1 resonance and the eight possible $a_1^\pm\pi^\mp$ combinations per event, wash out any differences between the two-pion invariant mass spectra of $a_1\pi$ and $\rho^0\pi^+\pi^-$ events. A search for the reaction $\gamma\gamma\to a_2(1320)^\pm\pi^\mp\to\rho^0\pi^\pm\pi^\mp$ was also performed in our data sample. However, it was found that, for $W_{\gamma\gamma}$ below 1.8 GeV/c^2, the Monte Carlo events generated according to $\rho^0\rho^0$ phase space reproduced the observed shape of the three-pion invariant mass spectra. Therefore, a non-zero amplitude for $a_2(1320)^\pm\pi^\mp$ is not required to describe our data.

VI Summary and conclusions

We have studied the reaction $\gamma\gamma\to\pi^+\pi^-\pi^+\pi^-$ and found a dominance of $\rho^0\rho^0$ production in the region below $W_{\gamma\gamma}=1.8$ GeV/c^2. The large value of the cross section below the nominal $\rho^0\rho^0$ threshold indicates a steep rise of the transition matrix element in the $W_{\gamma\gamma}$ region below 1.5 GeV/c^2. A 7 parameter spin-parity analysis of the four-pion final state has been performed. The cross section for $\gamma\gamma\to\rho^0\rho^0$ is found to be dominated by the partial waves $J^P=2^+$ with helicity 2. The inclusion of interference terms between 0^+ and $(2^+, 0)$ and between the 0^- and 2^- amplitudes (a 9 parameter fit) does not change this conclusion. A possible explanation for the disagreement among existing experimental results [3, 5, 6] for the ratio of the $(2^+, 2)$ and 0^+ amplitudes was investigated. It has been shown that small systematic or statistical errors in the determination of $|T_{(2^+,2)}|^2$ or $|T_{0^+}|^2$ may be the cause for the differences. A strong suppression of the helicity 0 contribution to the 2^+ amplitude with respect to helicity 2 is also observed. The contribution of negative parity states in the $\gamma\gamma\to\rho^0\rho^0$ reaction is small, in contrast to the large $\rho^0\rho^0$ yield with $J^P=0^-$ in radiative J/ψ decays [18].

It is interesting to compare our results with the results on the isospin related reaction $\gamma\gamma\to\rho^+\rho^-$ [7, 8]. The ratio of the cross sections is $\sigma_{\rho^0\rho^0}/\sigma_{\rho^+\rho^-}\simeq 4$. This result cannot be explained if only pure $I=0$ or $I=2$ states are produced, but implies that $I=0$ and $I=2$ states interfere constructively in the $\rho^0\rho^0$ and destructively in the $\rho^+\rho^-$ channel. The observed ratio of the cross sections and the dominance of one spin-parity state, $J^P=2^+$ with helicity 2, can be explained by a superposition of an $I=0$ and an exotic $I=2$ state with the same spin-parity quantum numbers. Such an interference pattern was predicted in [9] in the framework of the MIT bag model. This model predicts two degenerate four-quark states around 1.6 GeV/c^2 with $I=0$ and $I=2$ and spin parity $J^P=2^+$ which have super-allowed decays into $\rho\rho$ [19].

Acknowledgement. It is a pleasure to thank U. Djuanda, E. Konrad, E. Michel, and W. Reinsch for their competent technical help in running the experiment and processing the data. We thank Dr. H. Nesemann, B. Sarau, and the DORIS group for the excellent operation of the storage ring. The visiting groups wish to thank the DESY directorate for the support and kind hospitality extended to them.

References

1. TASSO Coll., R. Brandelik et al.: Phys. Lett. 97B (1980) 448
2. MARK II Coll., D.L. Burke et al.: Phys. Lett. 103B (1981) 153
3. TASSO Coll., M. Althoff et al.: Z. Phys. C – Particles and Fields 16 (1982) 13
4. CELLO Coll., H.J. Behrend et al.: Z. Phys. C – Particles and Fields 21 (1984) 205

5. TPC-2γ Coll., H. Aihara et al.: Phys. Rev. D37 (1988) 22; A. Buijs: Production of four-prong final states in photon-photon collisions. Ph.D. thesis, Utrecht University, Netherlands (1987)
6. PLUTO Coll., Ch. Berger et al.: Z. Phys. C – Particles and Fields 38 (1988) 521; H. Mueller: Messung und Analyse der Reaktion $\gamma\gamma \rightarrow \pi^+ \pi^- \pi^+ \pi^-$ mit PLUTO, Ph. D. thesis, Siegen University, Federal Republic of Germany (1987)
7. ARGUS Coll., H. Albrecht et al.: Phys. Lett. 217B (1989) 205
8. CELLO Coll., H.J. Behrend et al.: Phys. Lett. 218B (1989) 494
9. N.N. Achasov et al.: Phys. Lett. 108B (1982) 132; Z. Phys. C – Particles and Fields 27 (1985) 99; Phys. Lett. 203B (1988) 309; B.A. Li, K.F. Liu: Phys. Rev. Lett. 51 (1983) 1510; Phys. Rev. D30 (1984) 613; K.F. Liu, B.A. Li: Phys. Rev. Lett. 58 (1987) 2288; B.A. Li: Production of $Q^2 \bar{Q}^2$ states. SLAC-PUB-5007, 1989
10. G. Alexander et al.: Phys. Rev. D26 (1982) 1198; Z. Phys. C – Particles and Fields 30, (1986) 65; H. Kolanoski: Z. Phys. C – Particles and Fields 39 (1988) 543; J. Brodsky, G. Lepage: Phys. Rev. D24 (1981) 1808; J. Brodsky, G. Köpp, P. Zerwas: Phys. Rev. Lett. 58 (1987) 443
11. ARGUS Coll., H. Albrecht et al.: Nucl. Instrum. Methods A275 (1989) 1
12. ARGUS Coll., H. Albrecht et al.: Phys. Lett. 196B (1987) 101
13. M. Poppe: Int. J. Mod. Phys. A1 (1986) 545
14. L.I. Schiff: Quantum mechanics, p. 110, New York: McGraw-Hill 1955
15. J.D. Jackson: Nuovo Cimento 34 (1964) 1644
16. V.M. Budnev et al.: Phys. Rep. 15 (1975) 181
17. B. Boštjančič: Production of four pions in photon-photon reactions. Ph.D. thesis, University of Ljubljana, Ljubljana, 1990
18. MARK III Coll., R.M. Baltrusaitis et al.: Phys. Rev. D33 (1986) 1222
19. R.J. Jaffe: Phys. Rev. D15 (1977) 267; Phys. Rev. D15 (1977) 281